Original Article

Cardiac Magnetic Resonance Imaging In The Evaluation Of Patients With Valvular Heart Disease

1- Aalaa Yehia Mohammed Yehia , MSc. , 2- Rania Sobhy Abou khadrah, M.D. , 3- Noha Hosam El-Din Behairy, MD. , 4- Amr Mohammed El-Badry, MD. , 5- Hanan Mohamed Saleh El_Ahwal, MD.

[1]Assistant lecturer of Radiodiagnosis & Medical Imaging, Faculty of Medicine, Tanta University. Kafr El-Zayat, Gharbia governorate, Egypt. Email: Alaa.yehia@med.tanta.edu.eg
[2]Assistant professor of Radiodiagnosis & Medical Imaging, Faculty of Medicine, Tanta University. Tanta, Gharbia governorate, Egypt. Email : rania.abokhadra@med.tanta.edu.eg
[3]Professor of Radiodiagnosis & Medical Imaging, Faculty of Medicine, Cairo University. Cairo governorate, Egypt. Email: nohabehairy@gmail.com
[4]Professor of Radiodiagnosis & Medical Imaging, Faculty of Medicine, Tanta University. El-Santa, Gharbia governorate, Egypt. Email: amr.elbadri@med.tanta.edu.eg
[5]Professor of Radiodiagnosis & Medical Imaging, Faculty of Medicine, Tanta University. Tanta, Gharbia governorate, Egypt. Email: hanan.elahwal@med.tanta.edu.eg
Dr / Aalaa Yehia Mohammed Yehia
Corresponding author
Assistant lecturer of Radio-diagnosis, Tanta University, Faculty of Medicine.
El Gharbia, Kafr El-Zayat, Egypt
Email: Alaa.yehia@med.tanta.edu.eg.
DOI: 10.47750/pnr.2023.14.02.174

Abstract

Background: The main challenge that faces management of valvular heart disease is that no medical therapies are known to decrease disease progression, or the resulting adverse outcomes on cardiac function. Cardiac imaging is essential to evaluate disease development and progression. It plays an important role in identifying valve lesion/dysfunction and to assess its severity as well as its impact on the cardiac function. Cardiac magnetic resonance (CMR) imaging may help in the assessment of Valvular heart disease. Our study was interested in studying Valvular lesions of different underlying pathologies and different forms of the resulting valve dysfunction (stenosis and/or regurgitation. The aim of this work was to assess role of cardiac MRI as a non-invasive tool in the evaluation of patients with Valvular heart disease in correlation with echocardiography. **Methods:** This prospective study included 40 patients suspected clinically and diagnosed by echocardiography with valvular heart disease. All patients were subjected to ECG monitoring, echocardiography and renal function test (blood urea, serum creatinine, estimation of glomerular filtration rate 'eGFR') and cardiac MRI examination. **Results:** There was fair agreement between echocardiography and CMR regarding the diagnosis of aortic regurgitation with kappa agreement coefficient (K = 0.242). There was perfect agreement between echocardiography and CMR regarding the grading of mitral stenosis with kappa coefficient (K = 0.813). There was moderate positive correlation between CMR-derived LV-EDV and MR volume as well as CMR-derived AR volume. **Conclusions:** Cardiac MRI added significant value to the assessment of valvular heart disease. It allows non-invasive, comprehensive evaluation of both valve lesion and its impact on the relevant cardiac chambers. It plays an important role in the assessment of patients with valvular affection with underlying congenital heart disease. CMR complements echocardiography and sometimes adds more additional valuable information.

Keywords: Cardiac Magnetic Resonance, Valvular Heart Disease, echocardiography

Background:

Valvular heart disease (VHD) is a major contributor to loss of physical function, quality of life and longevity. The epidemiology of VHD varies around the world, with the functional and degenerative disease predominant in high-income countries, while rheumatic heart disease is predominant in low-income and middle-income countries [1].

Transthoracic echocardiography (TTE) is the first choice for imaging of valvular heart disease (VHD) due to its widespread availability, real-time test, provide information of hemodynamic effects in addition to being a bedside test. Other modalities, such as trans-esophageal echocardiography (TEE), computed tomography (CT) and magnetic resonance imaging (MRI), may have a supplementary role in the diagnosis and detection of severity, deciding the timing/type of treatment and/or interventional procedure, detection of post procedural complications, and prognostic predictions [2].

Cardiac magnetic resonance (CMR) imaging may help in the assessment of the four heart valves, with comprehensive approach to both valvular lesion and ventricle, providing the ability of free choice of image planes with flow and volumetric quantification and hence may allow to characterize the severity of each valve lesion, and visualize the surrounding outflow tracts and vessels [3].

Most diagnostic and prognostic data and guidelines depended on echo findings, we hoped to change this as more anatomical and functional data were obtained from CMR.

Our study was the first cardiac MR study performed in our institution to assess the Valvular lesions. The aim of this work was to assess role of cardiac MRI as a non-invasive tool in the evaluation of patients with valvular heart disease in correlation with echocardiography.

Methods:

This prospective study included 40 patients, suspected clinically and diagnosed by echocardiography with valvular heart disease, referred to MRI unit at the Department of Radiology and medical imaging of our institution during the period from October 2019 to May 2022. The study was approved by the Ethics Committee of our faculty. An informed written consent was obtained from the patients.

Exclusion criteria were hemodynamic instability, acute respiratory insufficiency, decompensated congestive heart failure, frequent ventricular arrhythmias, and acute cardiac ischemic events. Patients with implanted electric and electronic devices (cardiac pacemaker, implantable defibrillator, cerebral aneurysm clip, neural stimulator, any type of ear implant, metallic ocular foreign body, implanted insulin pump, drug infusion device).

All patients were subjected to complete history taking (present, past and surgical history), clinical examination (general and local examination), ECG monitoring, echocardiography and renal function test (blood urea, serum creatinine, estimation of glomerular filtration rate 'eGFR') and cardiac MRI examination.

Technique of CMR imaging:

Before the examination, the heart rate and rhythm were evaluated. Patients were informed to remain motionless during the exam and were told that the system generates some loud noise. Two Children needed sedation with the use of chloral hydrate with dose adjustment under supervision of paediatrician. Cooperative patients were asked to avoid excessive swallowing, and to keep respiration as regular as possible, avoiding large diaphragmatic movements (sighs, cough, etc.). Cooperative patients were evaluated for the ability of breath-withholding for reasonable time; they were asked to perform a deep inspiration followed by expiration with end-expiratory breath holding. During this trial, the patient was observed for compliance and the ECG for significant changes. Male patients were instructed to shave chest skin hair for optimal impedance of ECG leads to skin. Patient's weight and height were also measured to calculate the body surface area (BSA) according to Du Bois formula: $BSA = 0.007184 \times \text{weight (Kg)}^{0.425} \times \text{height (cm)}^{0.725}$.

Magnetic resonance scanner

A closed MRI machine 1.5-T magnet (Signa Excite HD; GE Healthcare, Milwaukee, USA) and 1.5-T MR system (Aera®, Siemens AG Healthcare, Erlangen, Germany) were used.The patients were asked to lie on the MRI table in supine position, with head-first position. Four ECG pads were placed on the anterior chest wall, the first was placed 1 cm to the left of the xiphisternum, the second and the third were placed in such a way that they were aligned at 90° to each other where the first electrode forms the right angle and the distance between the electrodes 15 cm. The

fourth electrode was placed above the first electrode. The ECG was then checked for the QRS complex, adjustments of the site of the leads was done accordingly. The patient's heart rate was also detected on MRI monitor.
The respiratory sensor was placed over the maximum area of respiratory movement (abdomen or thorax) under the coil. A strap was used to fix the sensor.

Cardiac MRI protocol and standard parameters:

Child patients received 20-gauge intravenous line while elderly and adult patients received 18-gauge intravenous line to allow administration of the contrast agent. Localizer images in the three orthogonal planes (axial, sagittal and coronal) were obtained during free breathing and not gated to the ECG in order, using real-time interactive planning (FOV 450 X 450 mm^2, slice thickness 10 mm, gap 2 mm, TR/TE 4.1/1.8, and flip angle 50°, matrix 256 x 128). ECG gated, balanced steady-state free-precession, white blood cine images were acquired in standard trans-axial (chest) view, two-chamber, four-chamber, short-axis views, LVOT as well as RVOT. Images were acquired with MR imaging parameters as following: TR/TE: 4.2/1.8 ms, FOV: 380 x 380 mm^2, Matrix: 256x192, Slice thickness: 8mm, no gap, Phases: 25, Slice number: 8-11, SNA: 1, Flip angle: 60°, Scan Time: 0.07-0.12 sec.
Direct planimetry of the valve orifice (en-face cine view) was performed in case of valve stenosis, either aortic, pulmonary or mitral stenosis, direct planimetry of the valve orifice was obtained at the level of the valve tips. Multiple, thin slices (4–5 mm slice thickness) parallel to the valve were acquired with the use of 0 slice gap between consecutive slices.
Flow images were performed via velocity encoded gradient echo imaging (VENC), also known as phase contrast imaging in order to quantify the flow (the aortic and pulmonary flow). At first, in-plane flow image was acquired along the direction of blood flow, coping the image position from the previously obtained cine image. Velocity encoding sensitivity (VENC) was adapted to the expected velocities (Starting from 200 cm/sec for aortic flow and 150 cm/sec for pulmonary flow and increased by 50 cm/sec until there is no aliasing). After that, through plane images were acquired, aligned perpendicular to the expected main blood flow direction over the valves, located at the level of the opening of the valve orifice in the aortic root and proximal pulmonary trunk for each sequence. (VENC: 150-400 cm/sec, (adjusted as previously mentioned to avoid aliasing), FOV 320 x 320 mm^2, slice thickness of 5 mm, no gap, TR/TE 4.9/2.9 msec and flip angle 15°, matrix 256 x 128. The potential for background phase errors was reduced by placing the region of interest at iso- center of the magnet. Image data acquisition was gated to the ECG signal with a temporal resolution of 30 phases per cardiac cycle. Navigator-based non-breath hold techniques were applied to improve the temporal or spatial resolution.
Late gadolinium enhancement sequence was performed. The gadolinium-chelate contrast material; gadopentetate dimeglumine (Magnevist; Schering, Berlin, Germany) was given intravenously at a dose of 0.1-0.2 mmol/kg. Images were obtained in dynamic phases as following: 5 minutes after contrast administration, the lock locker sequence was performed (in short axis view) to assess the inversion time (TI) which was important to null the signal intensity of normal myocardium after the administration of the contrast agent. 10 minutes after contrast administration, late gadolinium enhancement images were acquired in contiguous short-axis imaging planes (from base to apex) and in a long axis imaging plane during end-expiration breath hold with a segmented inversion-recovery gradient echo sequence (black blood images). MR imaging parameters included: TR/TE: 7.4/3.4, FOV: 380 x 380 mm^2, TI: 250-400, Flip angle: 15^o, Matrix, 128x128, Slice thickness: 8mm, no gap. TI times were increased by 10 – 15ms every 2 minutes, to obtain maximal nulling of remote normal LV myocardium as the correct TI for "nulling" of normal myocardium slowly changes over time.

Image analysis and interpretation:

Images were transferred to commercially available workstation for post-processing and image analysis. Images were transferred to the off-line workstation; all images were analysed using CVi42® post-processing software version 5.6.6 (Circle Cardiovascular Imaging Inc., Calgary, Alberta, Canada). The freely available software Segment version 2.0 R4265 (http://segment.heiberg.se) was also used [4], and quantitative image analysis was performed using Matlab. Three observes with at least 5 years of experience in CMR imaging reviewed the images and wrote the reports in consensus.

Statistical analysis

The collected data were organized, tabulated and statistically analysed using SPSS Package 21 for Microsoft Windows. Shapirow Wilk test was done to test the normality of the quantitative data. Quantitative data were presented as mean, SD, Range and qualitative ones as number and percentage. For qualitative variables, Chi-square test was used for analysis and when it was found inappropriate, it was replaced by Fischer Exact or Monte Carlo exact test. Correlations between different variables were done using Spearman correlation coefficients. Spearman correlation was done between non-parametric variables. Kappa agreement was performed to measure the agreement between the main parameters of CMR and trans-thoracic echocardiography. A two tailed P value < 0.05 was considered statistically significant.

Results:

The present study included 40 patients presented with valvular heart disease based on clinical and echocardiographic diagnosis. The study included 24 males (60 %) and 16 females (40 %) with the age ranged from 5 years to 78 years (mean age 36 years) ± 18.6 SD.

The mitral valve was affected in 67.5% (27 patients), the aortic valve was affected in 37.5% (15 patients), the pulmonary valve was affected in 17.5% (7 patients), and the tricuspid valve was affected in 47.5 % (19 patients).

Regarding the aetiology of valvular heart disease, the study included 43 % (17 patients) caused by congenital heart disease, 57 % (23 patients) caused by acquired heart disease which included 43 % (17 patients) caused by rheumatic heart disease, 7 % (3 patients) caused by calcific aortic valve disease (CAVD) and other 7 % (3 patients) had valvular affection secondary to ischemic heart disease (IHD)

There was moderate agreement between CMR and echocardiography as regard the grading of mitral regurgitation with k=0.571 and there was perfect agreement between echocardiography and CMR regarding the grading of mitral stenosis with kappa coefficient (K = 0.813) (Table 1).

There was fair agreement between echocardiography and CMR regarding the diagnosis of aortic regurgitation with kappa agreement coefficient (K = 0.242) and there was no agreement between echocardiography and CMR regarding the diagnosis of aortic stenosis with k agreement coefficient= 0.000 (Table 2).

Moderate correlation was found between CMR and echocardiography as regard the measurements of AVA with Spearman rank correlation coefficient (rs) = 0.548 with no significant association between both, p value = 0.065 with CMR overestimated AVA than echocardiography in most cases. As regard the peak systolic velocity, moderate correlation was found between CMR and echocardiography as regard the measurements of peak systolic velocity with Spearman rank correlation coefficient (rs)= 0.427, with no significant association between both, p value = 0.166. Figure 1

Left atrial area was evaluated in the studied 40 patients and then was indexed to the body surface area in each patient. It ranged from 5.5 – 30 cm^2/m^2 with a mean of 18.8 cm^2/m^2 ± 7.69 SD. It was found to be average in 62.5 % (25/40 patients) while dilated in 37.5 % (15/40 patients), all of them had mitral valve pathology either primary or secondary; 53.3 % (8/15 patients) had double mitral lesion, 26.6 % (5/15 patients) had isolated mitral regurgitation and 6.6 % (1/15 patient) had isolated mitral stenosis and 6.6 % (1/15 patient) had mitral annular disjunction.

There was moderate positive correlation between CMR-derived mitral regurgitation volume and indexed left atrial area, Spearman rank correlation coefficient (rs) = 0.560 with significant association between both (P value=0.004).

Forty-five percent (18 patients) showed left ventricular dilatation with increased volumes denoting long standing volume overload with LV remodelling. There was moderate positive correlation between CMR-derived AR volume and LV-EDV, Spearman rank correlation coefficient (rs) = 0.558 with significant association between both (P value=0.038). There was moderate positive correlation between CMR-derived MR volume and LV-EDV, Spearman rank correlation coefficient (rs)= 0.531 with significant association between both (P value=0.006) Figure 2.

Left ventricular systolic function was assessed via quantification of left ventricular ejection fraction (LVEF). It ranges from 21-80% with mean of 53.5%±14.69 SD then patients were classified according to the American College of Cardiology (ACC) into; hyper-dynamic systolic function (5 % of the studied group of patients), normal systolic function (72.5 %), mild systolic dysfunction (5%), moderate dysfunction (7.5 %), and severe dysfunction (10%). Among the 15 patients presented with aortic valve disease, 33.3 % showed abnormal LV systolic function while among the 27 patients presented by mitral valve disease, 33.3 % showed abnormal LV systolic function.

Left ventricular mass was assessed by CMR; it ranged from 48-319 gm with a mean of 132.7 gm ± 67.72 SD. It was increased above normal representing LV hypertrophy in 25 % (10 patients); 4 of them had moderate aortic stenosis, 5 of them had severe aortic stenosis and 1 patient had severe LVOT obstruction by sub-aortic membrane.

Tricuspid valve disease represented 47.5 % (19/40 patients). All of them showed tricuspid valve structural abnormality. Tricuspid valve structure assessment included evaluation of valve leaflets morphology, leaflet mobility, cusp thickness and cusp calcification. Moderate agreement between echocardiography and CMR regarding the grading of tricuspid regurgitation was found with K = 0.436 (Table 3).

Pulmonary valve disease represented 17.5% (7/40patients). All those 7 patients showed pulmonary valve structural abnormality. Pulmonary valve structure assessment included evaluation of valve leaflets morphology, leaflet mobility, cusp thickness and cusp calcification**.** Moderate agreement between echocardiography and CMR regarding the diagnosis of pulmonary regurgitation with K = 0.538**.** Regarding the diagnosis of pulmonary stenosis (PS), 10 % (4/40 patients) were referred by echocardiographic diagnosis of pulmonary stenosis; all of them (4 patients; 100 %) were graded as severe degree of PS by CMR as well.

The right ventricular volumes were evaluated by CMR in the studied 40 patients, RV end-diastolic volume ranged from 56-410 ml with a mean of 173.2 ml ± 69.53 SD, RV end-systolic volume ranged from 11 – 189 ml with a mean of 79.2 ml ± 39.47 SD, RV stroke volume ranged from 31 - 221ml with a mean of 94.7 ± 39.51 SD

There was a statistically significant difference between patients with tricuspid valve affection and those with normal tricuspid valve as regard RV volumes (P value = 0.028). Also, there was a statistically significant difference between patients with pulmonary valve affection and those with normal pulmonary valve as regard RV volumes (P value= 0.001) Table 5.

There was moderate positive correlation between CMR-derived TR volume and RV-EDV, Spearman rank correlation coefficient (rs) = 0.520 with significant association between both (P value=0.027) while there was a weak positive correlation between CMR-derived pulmonary regurgitation volume and RV-EDV, Spearman rank correlation coefficient (rs) = 0.319 with no significant association between both (P value = 0.538).

Right ventricular systolic function was assessed via quantification of right ventricular ejection fraction (RVEF). It ranged from 27-80% with mean of 55.5 % ± 11.38 SD; then patients were classified according to the American College of Cardiology (ACC) into; hyper-dynamic systolic function (2.5 % of the studied group of 40 patients), normal systolic function (70 %), mild systolic dysfunction (20%), moderate dysfunction (5 %), and severe dysfunction (2.5%). Among the 19 patients presented by tricuspid valve disease, 31.5 % (6/19 patients) showed RV systolic dysfunction, and among the 7 patients presented by pulmonary valve disease, 57.2 % (4/7 patients) showed mild RV systolic dysfunction.

There was no statistically significant difference between patients with normal tricuspid valve and others with tricuspid valve disease as regard RV systolic function while there was statistically significant difference between patients with normal pulmonary valve and others with pulmonary valve disease as regard RV systolic function (P value= 0.026) Table 5.

Discussion

Valvular heart disease (VHD) is a significant and increasing global problem. In the developing world, the primary sufferers are children and young adults, advances in technology have allowed precise definition of the structural and functional abnormalities of VHD, enabling etiologic classification of VHD in vivo [4-5,6].

As regarded to AS 5 % (2 patients) presented with sub-aortic stenosis caused by sub-aortic circumferential fibrous membrane. One of these two patients represented recurrent sub-aortic membrane associated with past history of previous membrane resection with aortic valve. This goes in concordance with Saef et al., [7] who stated that amongst children recognized to have obstructive congenital LVOT lesions, 71–77% have aortic valvular stenosis, 10–14% have sub-valvular stenosis, and 0–8% have multi-level obstruction. Sub-valvular or sub-aortic stenosis (SAS) comes in many forms, with the most common being a thin, discrete, fibrous, circumferential membrane within the outflow tract that is attached to the ventricular septum. It has been found to recur after surgical removal.

Seventeen patients presented with rheumatic heart disease (RHD) in the present study, 88.2 % (15/17 patients) showed mitral valve affection, followed by the aortic valve which was affected in 35.3 % (6/17patients), then the tricuspid valve was affected by RHD in 23.5 % (4/17 patients). This agreed with Manjunath et al, [8] who reported that in RHD, the order of involvement of valves is the mitral valve followed by aortic, tricuspid and pulmonary valves with the overall involvement of mitral valve in RHD to be 84.7%.

The present study included 22.5 % (9 patients) presented with mitral stenosis (MS) and 60 % (24 patients) presented with mitral regurgitation (MR), (17/24) had isolated MR and 7/24 patients had combined stenosis and regurgitation. Mitral stenosis was only of rheumatic aetiology in our study. This agreed with Manjunath et al [8].

Our study showed moderate agreement between CMR and echocardiography as regard the degree of mitral regurgitation with k=0.571. This agreed with a study conducted by Heitner et al., [9] which reported moderate agreement between MR as graded by cine-CMR and echocardiography [kappa=0.47 (0.29–0.65)].

As regarded to MR, echocardiography reported 4 cases with severe MR and CMR reported only 1 of them as severe MR and the other 3 patients were reported as moderate MR. This was consistent with Botis et al., [10] and Myerson [3], who reported that moderate MR on CMR is usually overestimated by TTE.

As regard the diagnosis of mitral stenosis, 9 patients had the diagnosis of mitral stenosis based on the measured mitral valve area (by direct planimetry) and the estimated mean pressure gradient and they were graded as mild, moderate, and severe with perfect agreement between both modalities (echocardiography-CMR) with (K = 0.813, P = 0.002). This agreed with Helvacioglu et al., [11] that showed very strong agreement between CMR and echocardiography. Rheumatic heart disease was the only underlying pathology in the present study. This agreed with Almeida et al., [12 .

CMR in our study allowed detailed assessment of the aortic valve anatomy and structure and enabled to differentiate congenital from acquired pathology (3 patients had bicuspid aortic valve and 1 patient had uni-cuspid valve). This agreed with Cawley et al., [13] who mentioned that CMR has the potential to visualize all parts of the valve leaflets throughout the entire cardiac cycle. .
One out of the two patients who had sub-aortic membrane, revealed concomitant recurrent moderate aortic stenosis for which the patient previously underwent balloon valvuloplasty. This was consistent with Cavalcante et al., [14] who mentioned that one of the advantages of CMR imaging is the ability to identify the site of flow acceleration, differentiating sub-valvular from valvular or supravalvular stenosis.

Direct quantification of aortic regurgitation (AR) by CMR in our study was performed via phase-contrast velocity mapping which enabled to quantify aortic regurgitation volumes and fractions and then, patients were graded as having mild, moderate, or severe aortic regurgitation. We found a fair agreement between echocardiography and CMR regarding the grading of aortic regurgitation with kappa coefficient (K = 0.242, P value= 0.001). This was similar to Haberka et al., [15] who found that the inter-modality agreement (TTE-CMR) in AR grading across mild, moderate and severe AR was low ($\kappa = 0.15$).

We measured the aortic valve area (AVA) by CMR via direct planimetry in the 12 patients diagnosed to have aortic stenosis, it ranged from 0.5 cm^2 to 1.4 cm^2. There was moderate correlation between CMR and trans-thoracic echocardiography (TTE) as regard the aortic valve area with (rs=0.548 & p<0.065). Also, moderate correlation between CMR and trans-thoracic echocardiography (TTE) as regard the peak systolic velocity with (rs=0.427 &

p<0.166). This was in line with De Rubeis et al., [16] who found that PC-MRI shows a high degree of correlation (Pearson's correlation coefficient from 0.61 to 0.81) regarding flow derived parameter (mean and peak velocity and gradient, AVA) with respect to TTE.
No agreement was found between CMR and echocardiography as regard the grading of aortic stenosis (K=0.000). CMR underestimated the degree of aortic stenosis in 3 patients (The peak velocity was <4 cm/sec and the AVA was > 1 cm^2). This agreed with Bohbot et al., [17] who stated that the direct planimetry of the stenotic aortic valve is prone to measurement errors, especially in case of nonplanar orifice or severe calcified AS, which can cause signal void and make border discrimination of the valve leaflets difficult. Furthermore, ECG gating may be a source of degrading image quality in patients with arrhythmias. Echocardiography did not report recurrent moderate aortic stenosis (AS) which was found in conjunction with severe sub-aortic stenosis owing to sub-aortic membrane. This was consistent with Myerson, [3] who stated that the excellent visualization of aortic outflow tract anatomy provides a good qualitative assessment of aortic valve function and easy identification of any sub-valvular or supravalvular stenosis.

In the present study, moderate positive correlation between CMR-derived volume and LV-EDV was found with (rs= 0.558, P =0.038). This agreed with Capron T. et al., [18 who found that there is significant correlation between LV-EDV and MR volume with (rs =0.65, P =0.0001).

In our study myocardial replacement fibrosis was assessed via LGE-CMR and evidence of late gadolinium enhancement was found in 4 of them (40 %) presented primarily with aortic valve disease (moderate or severe AS) and it was in the form of focal mid-wall patchy enhancement. This was in line with Bohbot et al., [17] who concluded that focal myocardial fibrosis is a frequent finding in patients with AS usually with a mid-wall scar pattern different from that of myocardial infarction and is associated with increased myocardial injury, diastolic and systolic dysfunction and adverse outcomes. There was evidence of late gadolinium enhancement in a patient presented with repaired tetralogy of Fallot (TOF). This agreed with Harris et al., [19] who stated that delayed-enhancement imaging detects fibrous tissue along regions of reconstruction in patients who have had surgery for congenital heart disease such as TOF.

Moderate positive correlation between CMR-derived mitral regurgitation volume and indexed left atrial area was found in our study with significant association between both (rs = 0.560, P = 0.004). This goes in line with Cameli et al., [20] who stated that in mitral regurgitation (MR), LA enlargement is a part of pathophysiological changes: it compensates the volume overload but is also a marker for future heart failure, atrial fibrillation and mortality after surgery. In the present study, 3/15 patients with LA dilatation, had double aortic lesion with moderate or severe AS together with left ventricular hypertrophy. This well matched with Saeed et al., [21] who mentioned that in aortic stenosis (AS), chronic pressure overload on the LV leads to LV hypertrophy, impaired relaxation, increased chamber stiffness, fibrosis, and LA dilatation. An enlarged LA may be a marker of longstanding diastolic dysfunction and more advanced disease in AS.

Two out of four patients who presented with congenital abnormality directly involving the tricuspid valve were presented with Ebstein anomaly and this was similar to what was mentioned by Hösch et al., [22] who reported that Ebstein anomaly constitutes about 40% of congenital TV malformations.

We found also in this study , 6/13 patients presented with secondary tricuspid regurgitation (TR) primarily had repaired congenital heart diseases complicated with RV pressure and/or volume overload resulting from pulmonary stenosis and/or pulmonary regurgitation (4 patients had repaired tetralogy of Fallot, 1 patient had Rastelli operation for TGA and 1 patient had pulmonary valvuloplasty for congenital PS). This was consistent with Driessen et al., [23] who stated that tricuspid valve regurgitation (TR) frequently complicates congenital heart defects (CHD) associated with right ventricular (RV) pressure or volume overload. The presence and severity of TR in those patients is independently associated with both increased morbidity and increased mortality. Our findings showed moderate agreement between CMR and echocardiography as regard the degree of tricuspid regurgitation with (k=0.436, P=0.014). This agreed with a study conducted by Medvedofsky et al., [24] which reported moderate agreement between echocardiography and the conventional CMR methodology in TR quantification [[kappa=0.55].

As regarded to pulmonary valve disease represented 17.5%in our study. All those patients had the underlying pathology as congenital heart disease (CHD) associated with pulmonary stenosis either isolated (in only 1 patient) or as a part of the complex CHD (in 6 patients). 71.5% (5/7 patients) primarily had tetralogy of Fallot associated with pulmonary stenosis as one of its main pathological components. All of them underwent previous intervention and presented with residual/recurrent pulmonary lesion. Two patients presented with severe stenosis of the RV/MPA valved conduit together with mild or moderate pulmonary regurgitation. Other two patients presented with moderate or severe free pulmonary regurgitation following trans-annular patch that aimed to relieve the previous pulmonary stenosis. One patient still had severe pulmonary valvular and supra-valvular stenosis (with the previous intervention was modified Blalock-Taussing "MBT" shunt that aimed to increase the pulmonary flow) prior to definitive correction. This matched with Saremi et al., [25] .

In the present study, 1 patient presented with severe stenosis of the RV/MPA valved conduit combined with mild pulmonary regurgitation with previous history of Rastelli operation for correction of his status of transposition of great arteries (TGA) together with severe irresectable LVOT obstruction.

One of the studied patients presented with moderate pulmonary regurgitation following pulmonary balloon valvuloplasty for severe congenital pulmonary stenosis. Luo et al., [26] conducted a study to assess percutaneous balloon pulmonary valvuloplasty for critical pulmonary stenosis with short and medium term follow-up and stated that pulmonary valve regurgitation is found in 41-88% of cases undergoing pulmonary balloon valvuloplasty.

There was moderate agreement between CMR and echocardiography as regard the diagnosis of pulmonary regurgitation with K=0.538. This was consistent with Van Berendoncks et al., [27] who found moderate agreement between CMR and echocardiography as regard the 3 pulmonary regurgitation categories (mild, moderate and severe) with (kappa coefficient of agreement 0.465.

Seven patients in this study who presented with pulmonary valve pathology (whether stenosis and/or regurgitation) showed RV dilatation and there was statistically significant difference between patients with pulmonary valve pathology and others with normal pulmonary valve as regard RV volumes with (p value=0.001). Also, 57% showed mild RV systolic dysfunction with statistically significant difference between both groups (P=0.026). There was weak positive correlation between CMR-derived pulmonary regurgitation volume and RV-EDV (rs= 0.319) with no significant association between both (P value=0.538). This well-matched Śpiewak et al., [28] who found that neither PR fraction nor PR volume correlated with RV end-diastolic volume ($r = 0.36$; $p = 0.15$ and $r = 0.37$; $p = 0.14$, respectively, for pulmonary regurgitation volume and fraction.
We also found a moderate positive correlation between CMR-derived TR volume and indexed right atrial area (rs= 0.454) with no significant association between both (P=0.079). On the contrary, Offen et al., [29] found poor correlation between right atrial area and the degree of TR ($rs = 0.36$, $p < 0.01$).
In the present study, 2 patients showed QP/QS ratio > 1.5, denoting the presence of significant shunt (1 of them presented with un-repaired atrio-ventricular septal defect (AVSD) and the other patient presented with tetralogy of Fallot with MBT shunt insertion). 15% had history of previously repaired shunt and showed average QP/QS ratio (ranged from 1-1.2) denoting no residual shunt.

Limitations of the study: Number of study patients might not have been large enough to provide statistical significance, data demonstrating agreement and correlation with echocardiographic grading were provided, long scan time, suboptimal imaging in case of arrhythmia, and susceptibility to respiratory artifacts also represented some limitations in the current study.

Conclusions:

Cardiac MRI added significant value to the assessment of valvular heart disease. It allowed non-invasive, comprehensive evaluation of both valve lesion and its impact on the relevant cardiac chambers. It played an important role in the assessment of patients with valvular affection with underlying congenital heart disease. It was not restricted by body habitus, acoustic window, or geometric assumptions, thus CMR complemented echocardiography and sometimes add more additional valuable information.

List of abbreviation:

Ao (Aorta), AR (Aortic regurgitation), AS (Aortic stenosis), AVA (aortic valve area),AVSD (Atrio-ventricular septal defect), BAV (bicuspid aortic valve), BSA (body surface area),CHD (Congenital heart disease),CMR (cardiac magnetic resonance),CT (Computed tomography),

Echo (echocardiography), ECG (Electrocardiography),EDV ((End diastolic volume), EF (Ejection fraction), eGFR (estimated glomerular filtration rate),FOV (field of view), ESV (End systolic volume), EDVI (Indexed end diastolic volume), ESVI (Indexed end systolic volume), FOV (Field of view),K (Kappa agreement coefficient),LA (Left atrium), LGE (Late gadolinium enhancement), LV (Left ventricle),LVOT (left ventricular outflow tract), MAD (mitral annular disjunction),MR (mitral regurgitation), MS (mitral stenosis), MBT (Modified Blalock-Taussing shunt), MPA (Main pulmonary artery), PR (pulmonary regurgitation), PS (pulmonary stenosis), RHD (Rheumatic heart disease), rs (Spearman rank correlation coefficient), RV (Right ventricle),RVOT (Right ventricular outflow tract),SAS (Sub-aortic stenosis),TE (time of echo), TEE (trans-esophageal echocardiography),TGA (transposition of great arteries),TI (inversion time), TOF (Tetralogy of Fallot), TR (time of repetition),TR(Tricuspid regurgitation),TTE (trans-thoracic echocardiography),VA (ventricular arrhythmia),VENC (Velocity encoding)VHD (valvular heart disease)

References:

1. Coffey S, Roberts-Thomson R, Brown A, et al. Global epidemiology of valvular heart disease. Nat Rev Cardiol. 2021;18(12):853-864.
2. Zheng R, and Kusunose K. Review: Application of current imaging modalities in the management of left-sided valvular heart disease. Cardiovasc Diagn Ther. 2021;11(3):793-803.
3. Myerson SG. CMR in Evaluating Valvular Heart Disease: Diagnosis, Severity, and Outcomes. JACC Cardiovasc Imaging. 2021;14(10):2020-2032.
4. Tufvesson J. Hedstrom E, Steding-Ehrenborg K, et al. Validation and development of a new automatic algorithm for time-resolved segmentation of the left ventricle in magnetic resonance imaging. Journal of Cardiovascular Magnetic Resonance 2015; 17(1): 68.
5. Farrar EJ, and Butcher JT. Valvular heart diseases in the developing world: Developmental biology takes center stage. J Heart Valve Dis. 2012;21(2):234-240.
6. Boudoulas KD, Borer JS, and Boudoulas H. Etiology of valvular heart disease in the 21st century. Cardiol. 2013;126(3):139-152.
7. Saef JM, and Ghobrial J. Valvular heart disease in congenital heart disease: A narrative review. Cardiovasc Diagn Ther. 2021;11(3):818-839.
8. Manjunath CN, Srinivas P, Ravindranath KS, et al. Incidence and patterns of valvular heart disease in a tertiary care high-volume cardiac center: A single center experience. Indian Heart J. 2014;66(3):320-326.
9. Heitner J, Bhumireddy GP, Crowley AL, et al. Clinical application of cine-MRI in the visual assessment of mitral regurgitation compared to echocardiography and cardiac catheterization. PLoS One. 2012;7(7).
10. Botis I, Efstathiadou A, Papanastasiou CA, et al. Evaluation of mitral regurgitation by cardiac magnetic resonance and transthoracic echocardiography: a systematic review and meta-analysis. Rev Cardiovasc Med. 2021;22(4):1513-1521.
11. Helvacioglu F, Yildirimturk O, Duran C, et al. The evaluation of mitral valve stenosis: Comparison of transthoracic echocardiography and cardiac magnetic resonance. Eur Heart J Cardiovasc Imaging. 2014;15(2):164-169.
12. Azevedo D, Mancio J, Pessoa-Amorim G, et al. Left ventricular reverse remodeling and function by strain analysis in aortic stenosis: A CMR analysis of the EPICHEART study. Rev Port Cardiol. 2021;40(3):153-164.
13. Cawley PJ, Hamilton-Crai C, Owens DS, et al. Prospective comparison of valve regurgitation quantitation by cardiac magnetic resonance imaging and transthoracic echocardiography. Circ Cardiovasc Imaging. 2013;6: 48–57.
14. Cavalcante JL, Lalude OO, Schoenhagen P, et al. Cardiovascular Magnetic Resonance Imaging for Structural and Valvular Heart Disease Interventions. JACC Cardiovasc Interv. 2016;9(5):399-425.
15. Haberka M, Bałys M, Gąsior Z, et al. Aortic regurgitation and left ventricle remodeling on cardiac magnetic resonance and transthoracic echocardiography. Kardiol Pol. 2021;79(9):965-971.
16. De Rubeis G, Galea N, Ceravolo I, et al. Aortic valvular imaging with cardiovascular magnetic resonance: Seeking for comprehensiveness. Br J Radiol.2019;92(1101):9-13.
17. Bohbot Y, Renard C, Manrique A, et al. Usefulness of Cardiac Magnetic Resonance Imaging in Aortic Stenosis. Circ Cardiovasc Imaging. 2020;13(5):1-16.
18. Capron T, Cautela J, Scemama U, et al. Cardiac magnetic resonance assessment of left ventricular dilatation in chronic severe left-sided regurgitations: comparison with standard echocardiography. Diagn Interv Imaging. 2020;101(10):657-665.
19. Harris, M, Johnson R, Weinberg P. et al. Delayed-enhancement cardiovascular magnetic resonance identifies fibrous tissue in children after surgery for congenital heart disease. J. Thorac. Cardiovasc. Surg. 2007; 133 (3), 676-681.
20. Cameli M, Incampo E, and Mondillo S. Left atrial deformation: Useful index for early detection of cardiac damage in chronic mitral regurgitation. IJC Hear Vasc. 2017;17:17-22.
21. Saeed S, Rajani R, Tadic M, et al. Left atrial volume index predicts adverse events in asymptomatic moderate or severe aortic stenosis. Echocardiography. 2021;38(11):1893-1899.
22. Hösch O, Alt SC, Paul T, et al. Managing Ebstein's Anomaly of the Tricuspid Valve: Impact of Cardiovascular Magnetic Resonance. J Cardiol Ther. 2014;1(7):154-159.

23. Driessen MMP, Schings MA, Sieswerda GT, et al. Tricuspid flow and regurgitation in congenital heart disease and pulmonary hypertension: Comparison of 4D flow cardiovascular magnetic resonance and echocardiography. J Cardiovasc Magn Reson. 2018;20(1):1-10.
24. Medvedofsky D, Mor-Avi V, Kruse E, et al. Quantification of right ventricular size and function from contrast-enhanced three-dimensional echocardiographic images. J Am Soc Echocardiogry. 2017;30(12):1193–1202.
25. Saremi F, Gera A, Ho SY, et al. CT and MR imaging of the pulmonary valve. Radiographics. 2014;34(1):51-71.
26. Luo F, Xu W-Z, Xia C-S, et al. [Percutaneous balloon pulmonary valvuloplasty for critical pulmonary stenosis in infants under 6 months of age and short and medium term follow-up]. Zhonghua er ke za zhi = Chinese J Pediatr. 2011;49(1):17-20.
27. Van Berendoncks A, Van Grootel R, McGhie J, et al. Echocardiographic parameters of severe pulmonary regurgitation after surgical repair of tetralogy of Fallot. Congenit Heart Dis. 2019;14(4):628-637.
28. Śpiewak M, Petryka-Mazurkiewicz J, Mazurkiewicz Ł, et al. The impact of pulmonary regurgitation on right ventricular size and function in patients with repaired tetralogy of fallot and additional haemodynamic abnormalities. Polish J Radiol. 2020;85(1):e607-e612.
29. OffenSM,Baker D,Puranik R, et al. Right ventricular volum and its relationship to functional tricusped regurgitation. IJC Hear Vasc.2022;38:100940.

Figures' legend:

Figure 1: (A) a scatter-plot curve of correlation between aortic valve area measurements by CMR and echocardiography- spearman correlation in the group of patients diagnosed with AS, (B) a scatter-plot curve of correlation between trans-aortic peak systolic velocity measurements by CMR and echocardiography- spearman correlation in the group of patients diagnosed with AS.

Figure (2): (A) A scatter-plot curve of correlation between CMR-derived aortic regurgitation (AR) volume and left ventricular end-diastolic volume (LV-EDV)- spearman correlation in the 14 patients diagnosed with AR, (B) A scatter-plot curve of correlation between CMR-derived mitral regurgitation (MR) volume and left ventricular end-diastolic volume (LV EDV) - spearman correlation in the 24 patients diagnosed with MR

Figure (3): A 38-year-old female patient with chronic rheumatic heart disease, presented clinically with dyspnea, palpitation, and easy fatigability. It shows a high velocity jet of linear flow (high signal) surrounded by turbulence (low signal) (red arrow in **A**), fused commissures with restricted leaflet opening and aortic valve area = 0.6 cm^2, denoting severe stenosis **(B)**, the origin of the high velocity jet from the valve tips itself during systole (red arrow in **C & D**), contour placement for flow analysis (**E & F**), the regurgitation volume of about 17 ml (18 %), denoting mild regurgitation (**G**), signal void mitral regurgitation jet (red arrow in **H)**, thickened valve leaflets with restricted opening (yellow arrow **in I)**, mitral valve area (= 1.6 cm^2), denoting mild mitral stenosis **(J)**, average sized LV, increased mass and a hyper-dynamic systolic function and ventricular function analysis as follows: EDV=153 ml, ESV = 32 ml, SV= 121 ml, EF%= 79 %, and mass= 72 gm (Normal 70-142 gm according to age), mitral regurgitation volume (by indirect method) = 28 ml with (RF% = 23%), denoting mild regurgitation **(G & K)**, no coarctation of aorta **(L)**, and no myocardial scarring **(M)**. **Final CMRI diagnosis:** Confirmation of double aortic and mitral valve lesions, average LV volume with hyper-dynamic systolic function and exclusion of coarctation of the aorta

Figure (4): A 19-year-old male patient, presented clinically with dyspnea, decreased exercise tolerance with syncopal attacks. He had a past-history of aortic valvuloplasty with sub-aortic membrane resection 15 years ago. It shows a sub-aortic membrane (green arrow), 11 mm below the aortic valve (yellow arrow) during diastole **(A)**, high velocity, turbulent jet passing through the valve, being originating from the membrane just below the valve (red arrow in **B)**, the boundaries of the septal myocardium ( ) and anterior mitral leaflet (block arrow) define the area of sub-aortic membrane. The circumferential nature of the membrane is visualized as the mid-grey signals (short arrow) surrounding the orifice area as higher signals (long arrow) **(C)**, the measured aortic valve area= 1.1 cm^2, denoting moderate stenosis **(D)**, contour placement for trans-aortic flow analysis **(E & F)**, the regurgitation volume was about 8 ml (8.3%), denoting mild regurgitation **(G)**, contour placement on trans-membrane through plane flow images for flow analysis **(H & I)**, the maximum trans-membrane flow velocity was about 4.2 m/sec and the mean pressure gradient=70 mmHg ,denoting severe stenosis **(J)**, average sized LV, increased mass and average systolic function with ventricular function analysis as follows: EDV=180 ml, ESV = 76 ml, SV= 104 ml, EF%= 58 %, and mass= 120 gm (Normal 108-197 gm according to age) **(K)**, no coarctation of aorta **(L)**, and no evidence of delayed enhancement excluding myocardial fibrosis **(M)**. **Final CMRI diagnosis:** Recurrent sub-aortic membrane with subsequent severe sub-aortic stenosis, together with mild aortic regurgitation, average systolic function, and recurrent moderate aortic stenosis with exclusion of suspected bicuspid aortic valve and aortic coarctation.

Figure (5): A 37-year-old female patient with history of surgical repair of ASD 20 years ago and now planned for mitral valve surgery, presented clinically with dyspnea, fatigue, palpitation, and decreased exercise tolerance. It shows 2 signal void mitral regurgitation jets, one originating from the leaflets-coaptation site (block-white arrow) and the other from the anterior leaflet of mitral valve (red arrow),and markedly dilated left atrium (LAA=29.5 cm^2) **(A)**, a cleft is seen within the anterior mitral leaflet directed toward the septum (red arrow in **B & C)**, lack of offset of the septal leaflet of the tricuspid valve **(D)**, dilated LV, average mass and mildly impaired systolic function and ventricular function analysis as follows: EDV=213 ml, ESV = 127 ml, SV= 90 ml, EF%= 42 %, and mass= 95 gm (Normal 70-142 gm according to age), mitral regurgitation volume (by indirect method) =27 ml (32 %), denoting moderate regurgitation **(E & F)**, and enhancing closure patch being located at the most anterior and inferior aspect of the inter-atrial septum as well as at the inlet portion of interventricular septum **(G)**. **Final CMRI diagnosis:** Repaired ostium primum with mitral cleft, associated with moderate mitral regurgitation together with fibrosis at the site of closure patch (a post-repair of partial AVSD).

Figure (6): shows apical insertion of the septal leaflet (red arrowed S) of tricuspid valve for a distance of 2.6 cm **(A)**, the functional portion of the right ventricle (traced red in **B)**, the atrialized portion of the right ventricle (traced green in **C)**, the tethered inferior leaflet of tricuspid valve (red arrowed 'I' in **D)**, the signal void of tricuspid regurgitation jet (yellow arrow in **E)**, non-dilated functional portion of the right ventricle with average systolic function and ventricular function analysis was as follows: RV EDVI =89 ml/m^2, RV ESVI = 40 ml/m^2, RV-SVI= 49 ml/m^2 (RV-SV=100 ml), EF%= 54 % **(F)**, and no myocardium late gadolinium enhancement **(G)**. **Final CMRI diagnosis:** Ebstein anomaly with average volume and function of the functional portion of right ventricle and no evidence of myocardial fibrosis.

Tables' legend:

Table (1): Grading of mitral regurgitation and Kappa-agreement analysis for the grading of mitral regurgitation by CMR and echocardiography among the 24 patients diagnosed with mitral regurgitation, Grading of mitral stenosis by CMR, echocardiography and Kappa-agreement analysis for the grading of mitral stenosis by CMR and echocardiography among the 9 patients diagnosed with mitral stenosis.

Table (2): Grading of aortic regurgitation and Kappa-agreement analysis for the grading of aortic regurgitation by CMR and echocardiography in the group of 13 patients diagnosed with AR, Grading of aortic stenosis and Kappa-agreement analysis for the grading of aortic stenosis by CMR and echocardiography in the group of patients diagnosed with AS.

Table (3): Grading of tricuspid regurgitation and Kappa-agreement analysis for the grading of tricuspid regurgitation (TR) by CMR and echocardiography in the 19 patients diagnosed with TR.

Table (4): Grading of pulmonary regurgitation and Kappa-agreement analysis for the grading of pulmonary regurgitation (PR) by CMR and echocardiography in the 6 patients diagnosed with PR, Grading of pulmonary stenosis (PS) by echocardiography and CMR in the 4 patients diagnosed with PS**.**

Table (5): CMR-derived right ventricular volumes in the studied 40 patients, Relation between tricuspid valve function status and RV volume in the studied 40 patients, Relation between pulmonary valve function status and RV volume in the studied 40 patients, Relation between tricuspid valve function status and RV systolic function, between pulmonary valve function status and RV systolic function in the studied 40 patients and indexed right atrial area by cardiac MRI in the studied 40 patients.

Figure 3:

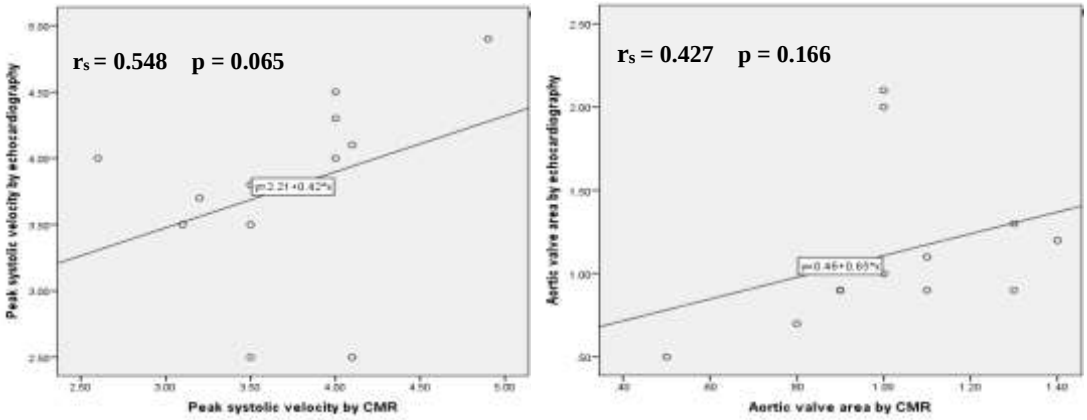

(A) (B)

Figure 2:

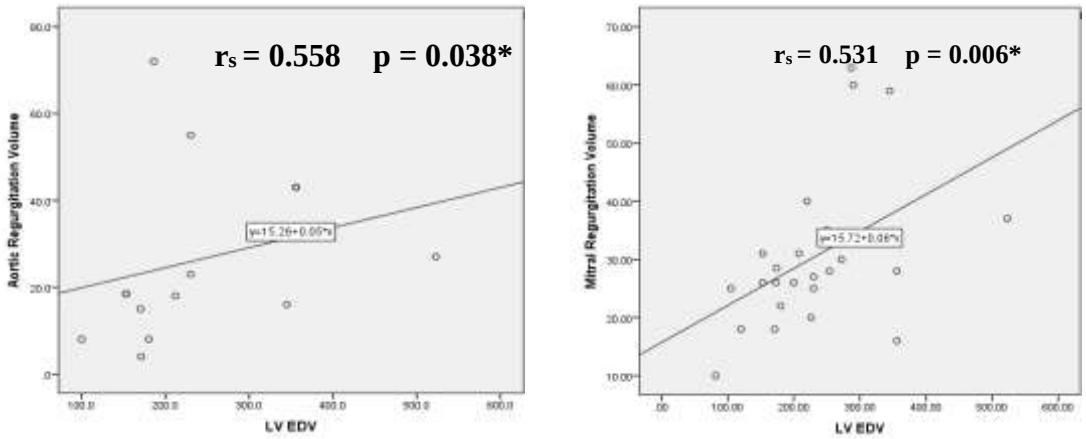

Figure 3

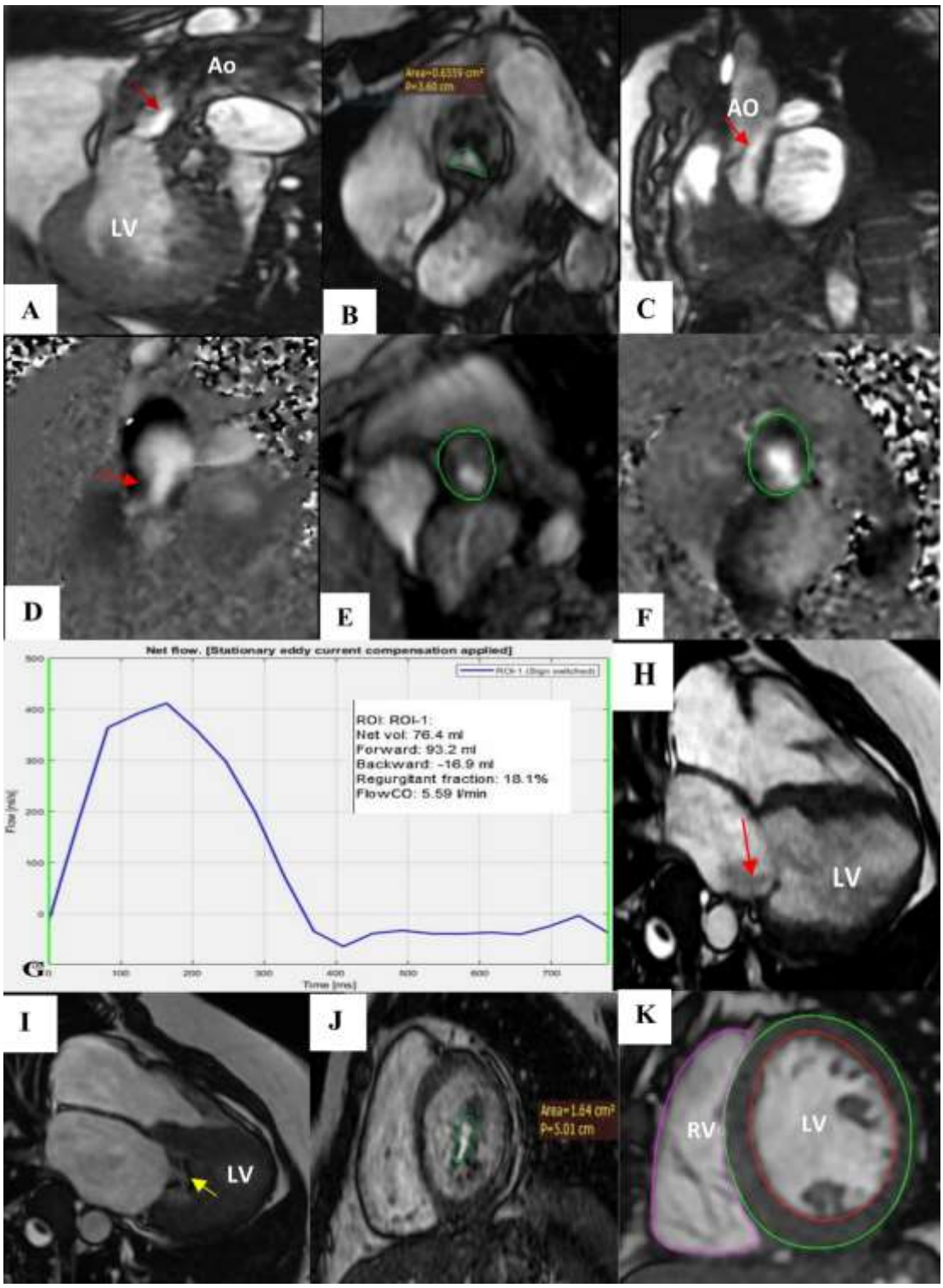
Ao
LV
A
B
AO
C
D
E
F
Net flow. [Stationary eddy current compensation applied]
ROI: ROI-1:
Net vol: 76.4 ml
Forward: 93.2 ml
Backward: -16.9 ml
Regurgitant fraction: 18.1%
FlowCO: 5.59 l/min
H
LV
I
LV
J
K
RV
LV

Figure 4:

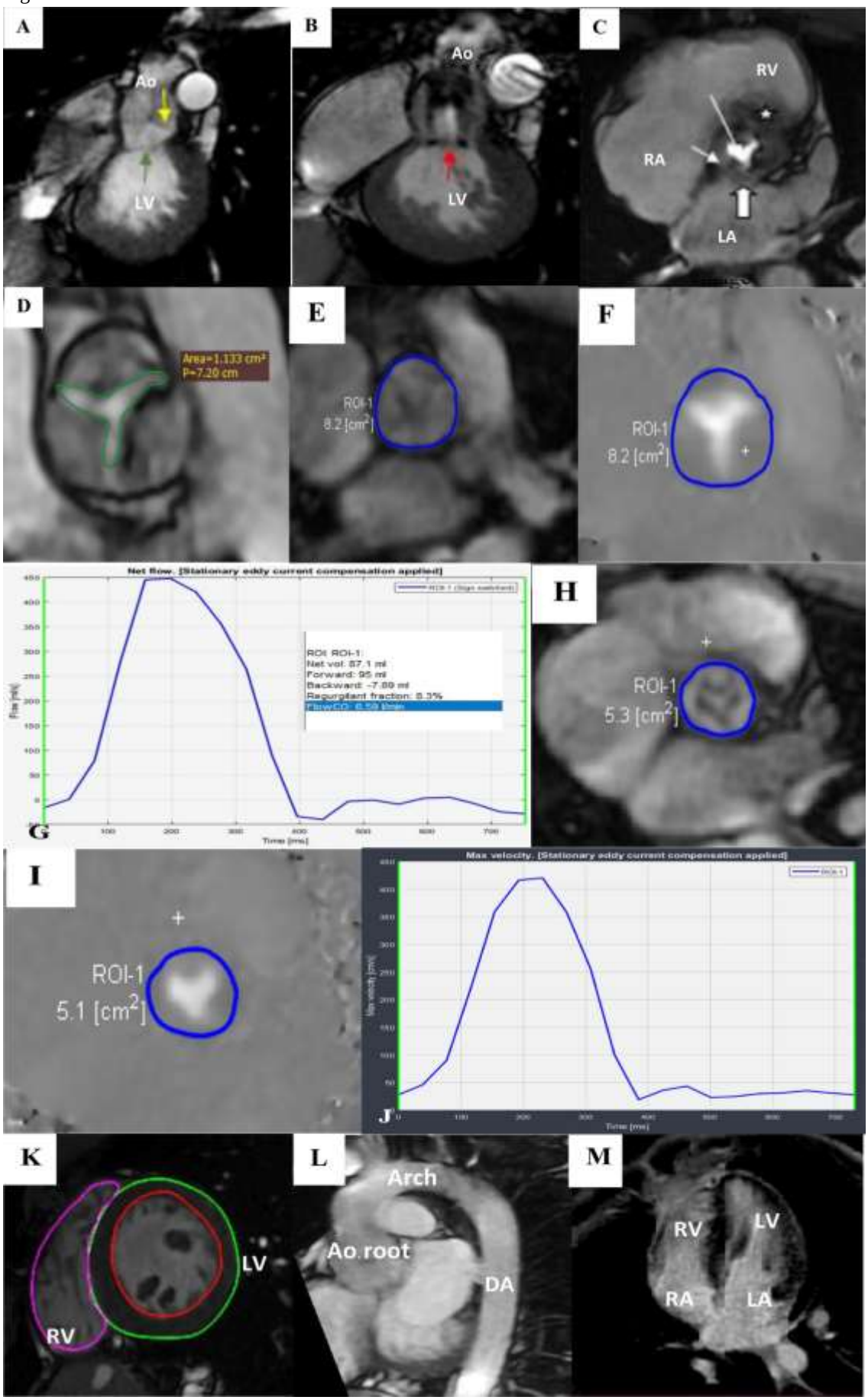
A
Ao
LV
B
Ao
LV
C
RV
RA
LA
D
Area=1.133 cm²
P=7.20 cm
E
ROI-1
8.2 [cm²]
F
ROI-1
8.2 [cm²]
Net flow. [Stationary eddy current compensation applied]
ROI: ROI-1:
Net vol: 87.1 ml
Forward: 95 ml
Backward: -7.89 ml
Regurgitant fraction: 8.3%
G
H
ROI-1
5.3 [cm²]
I
ROI-1
5.1 [cm²]
Max velocity. [Stationary eddy current compensation applied]
J
K
LV
RV
L
Arch
Ao root
DA
M
RV
LV
RA
LA

Figure 5:

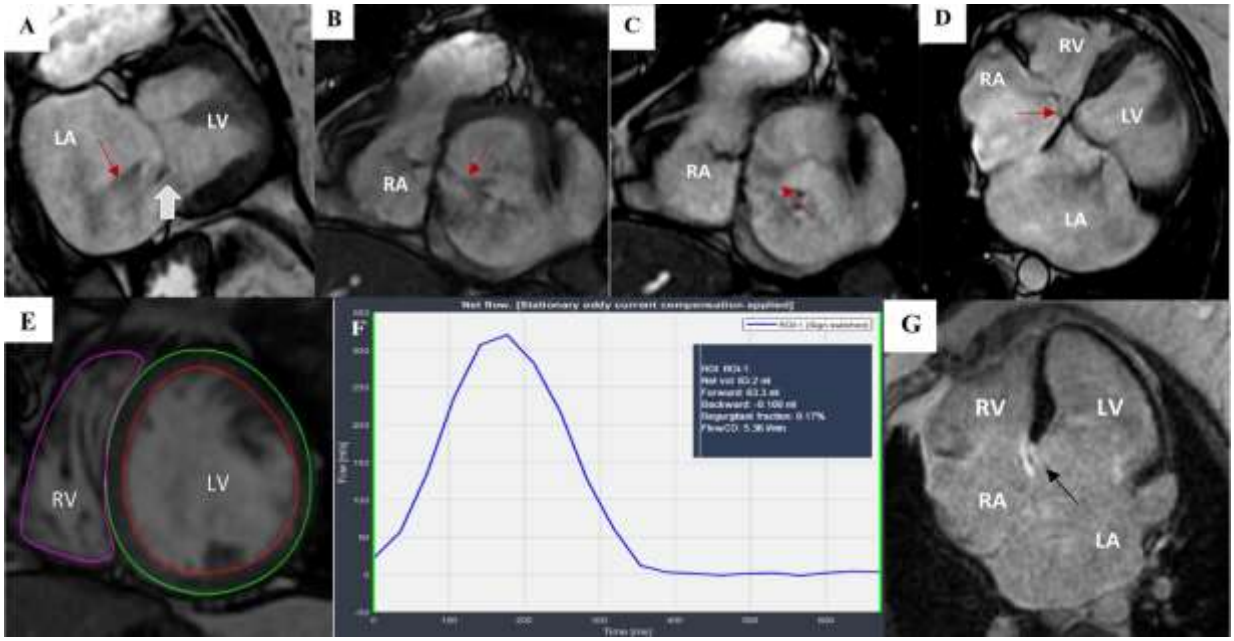

Figure 6:

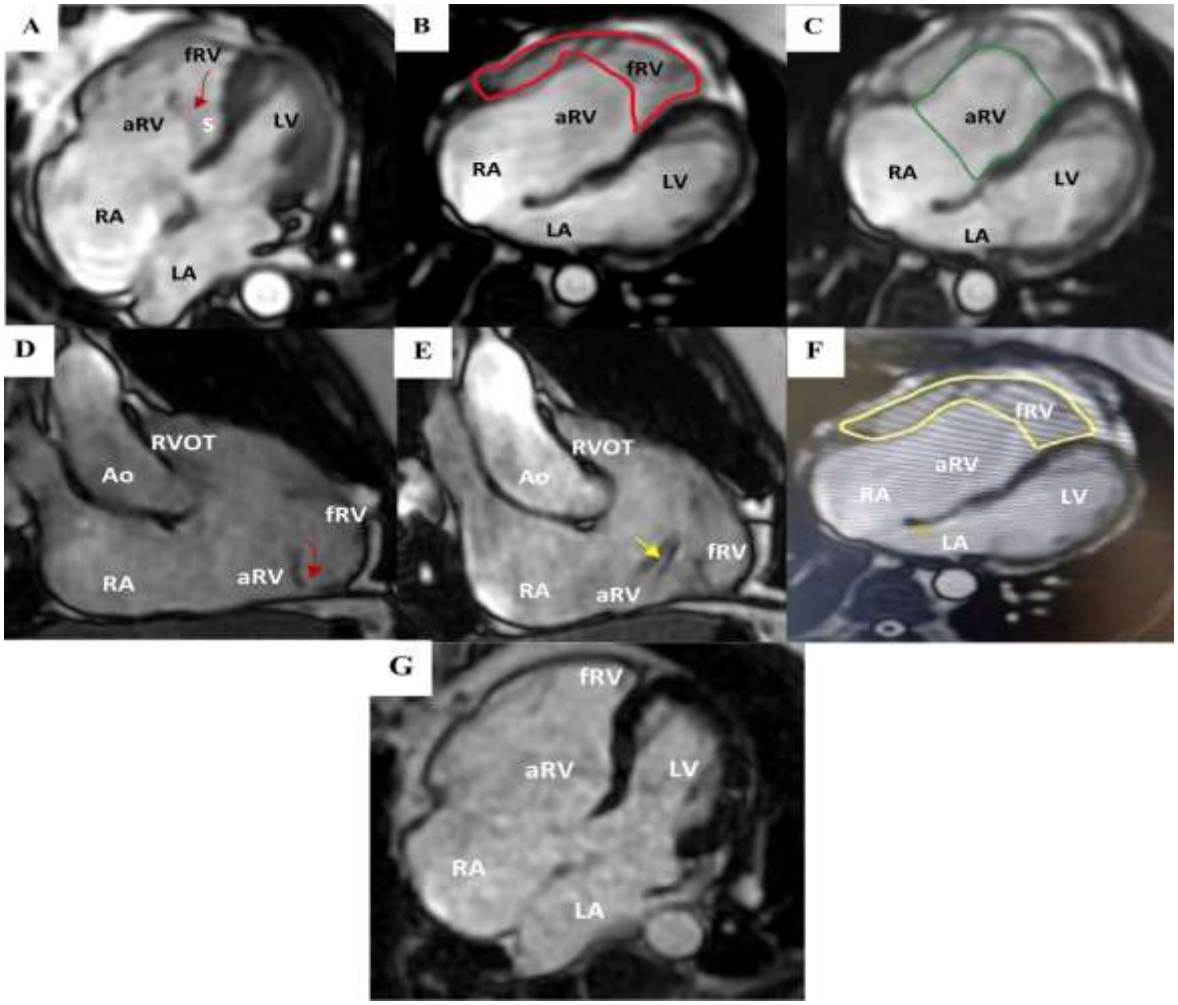

Table 1:

			By CMR		By echocardiography
Grading of mitral regurgitation		Mild	13(54.5%)		12(50.0%)
		Moderate	10(41.7%)		8(33.3%)
		Severe	1(4.2%)		4(16.7%)
		CMR			**Total**
Echocardiography		**Mild**	**Moderate**	**Severe**	
	Mild	11(84.6%)	1 (10.0%)	0 (0.0%)	12(50.0%)
	Moderate	2(15.4%)	6(60.0%)	0(0.0%)	8(33.3%)
	Severe	0(0.0%)	3(30.0%)	1(100.0%)	4(16.7%)
Total No. of patients		13(100.0%)	10(100.0%)	1(100.0%)	24(100.0%)
P = <0.001*					
			By echocardiography		**By CMR**
Grading of mitral stenosis	**Mild**		3(33.3%)		4(44.4%)
	Moderate		5(55.6%)		4(44.4%)
	Severe		1(11.1%)		1(11.1%)
Mitral valve area by CMR (mm^2)			1.5 ± 0.49		
Mean pressure gradient by CMR (mmHg)			4.8 ± 3.34		
			CMR		
			Mild	**Moderate**	**Severe**
Echocardiography	**Mild**		3(75.0%)	0(0.0%)	0(0.0%)
	Moderate		1(25.0%)	4(100.0%)	0(0.0%)
	Severe		0(0.0%)	0(0.0%)	1(100.0%)
P = 0.002*					

Data are presented as mean ± SD or frequency (%), *: significant as P value ≤ 0.05

Table 2:

			By echocardiography	**By CMR**
Grading of aortic regurgitation		**Mild**	7(53.8%)	8(57.1%)
		Moderate	3(23.1%)	2(14.3%)
		Severe	3(23.1%)	4(28.6%)
Aortic regurgitation volume by CMR (ml)		30.2 ± 23.91		
Aortic regurgitation fraction by CMR (%)		26.4 ± 19.75		
		CMR		
Echocardiography	**Mild**	6(85.8 %)	0(0.0%)	1(25.0%)
	Moderate	1(14.2%)	1(50.0%)	1(25.0%)
	Severe	0(0.0%)	1(50.0%)	2(50.0%)
K = 0.242 (Fair agreement)				

		By echocardiography	**By CMR**
Grading of aortic stenosis	**Moderate**	2(18.0%)	5(41.7%)
	Severe	9(82.0%)	7(58.3%)
Aortic valve area by CMR (mm^2)	1.0 ± 0.25		
Mean pressure gradient by CMR (mmHg)	55.7 ± 17.80		
Peak systolic velocity by CMR (m/sec)	3.7 ± 0.60		
	MRI		
	Moderate	**Severe**	
Echocardiography **Moderate**	1(25.0%)	1(0.0%)	
Severe	3(75.0%)	6(100.0%)	
Total No. of patients	4(100%)	7(100%)	
K = 0.000 (No agreement)			

Data are presented as mean ± SD or frequency (%),

Table 3:

			Echocardiography	**CMR**
Grading of tricuspid regurgitation		Mild	7 (31.6%)	5 (26.3%)
		Moderate	10 (47.4%)	12 (63.2%)
		Severe	2 (21%)	2(10.5%)
		Total No. of patients	19(100%)	19(100%)

		MRI			Total No. of patients
		Mild	Moderate	Severe	
Echocardiography	Mild	4(80.0%)	3(25.0%)	0(0.0%)	7(36.8%)
	Moderate	1(20.0%)	8(66.7%)	1(50.0%)	10(52.6%)
	Severe	0(0.0%)	1(8.3%)	1(50.0%)	2(10.5%)
Total No. of patients		5(100.0%)	12(100.0%)	2(100.0%)	19(100.0%)
K = 0.436 (Moderate agreement) P = 0.014*					

Table 4:

		By CMR
Grading of pulmonary regurgitation	Mild	2(33.3%)
	Moderate	3(50.0%)
	Severe	1(16.7%)
	Total No. of patients	6(100.0%)

		Mild	Moderate	Severe	Total No. of patients
Echocardiography	Mild	2(100.0%)	0 (0.0%)	0 (0.0%)	2(33.3%)
	Moderate	0 (0.0%)	1 (33.3%)	0 (0.0%)	1(16.7%)
	Severe	0 (0.0%)	2 (66.7%)	1(100.0%)	3 (50.0%)
		0.0%	66.7%	100.0%	50.0%
Total No. of patients		2(100.0%)	3(100.0%)	1(100.0%)	6(100.0%)
K = 0.538 (Moderate agreement) P = 0.021*					

Grading of pulmonary stenosis by echocardiography and CMR	Severe	4(100.0%)
Pulmonary valve area by CMR (mm^2)	0.8 ± 0.26	
Mean pressure gradient by CMR (mmHg)	55.7 ± 7.51	
Peak systolic velocity by CMR (m/sec)	3.6 ± 0.31	

Table 5:

		Tricuspid valve function	
		Normal	**Abnormal**
RV volume	**Average**	16(76.2%)	8(42.1%)
	Dilated	5(23.8%)	11(57.9%)
$\chi^2 = 4.829$ P = 0.028*			
		Pulmonary valve function	
		Normal	**Abnormal**
RV volume	**Average**	24(72.7%)	0(0.0%)
	Dilated	9(27.3%)	7(100.0%)
FE = 12.727 P = 0.001*			
		Tricuspid valve function	
		Normal	**Abnormal**
RV systolic function	**Normal**	16(76.2%)	13(68.4%)
	Mild dysfunction	5(23.8 %)	3(15.8%)
	Moderate dysfunction	0(0.0%)	2(10.5%)
	Marked dysfunction	0(0.0%)	1(5.3 %)
MC = 3.934 P = 0.453			
		Pulmonary valve function	
RV systolic function	**Normal**	25(75.7%)	3(42.8%)
	Mild dysfunction	4(12.1%)	4(57.2%)

	Moderate dysfunction	2(6.1%)	0(0.0%)
	Marked dysfunction	2(6.1%)	0(0.0%)
MC = 12.171 P = 0.026*			
		No. and percentage of patients	
Right atrial area indexed to BSA	**Average**	26(65.0%)	
	Dilated	14(35.0%)	
RAAI among studied patients	18.0 ± 6.24		
Upper normal limit of RAAI	22.7 ± 4.08		

Data are presented as mean ± SD or frequency (%), *: significant as P value ≤ 0.05, FE: Fischer Exact test, χ^2: Chi square test, MC: Monte Carlo Exact test,